

A Hall-effect sensor based instrument for measuring the door-seal gap of heavy trucks on the production line

Daniel P. Koch

*Department of Mechanical Engineering (Undergraduate)
Brigham Young University
Provo, Utah 84602
Email: daniel.p.koch@gmail.com*

Abstract

A proof-of-concept design for an instrument to measure the door-seal gap width on heavy trucks is presented. The door-seal gap is an important specification because if it is too small, the seal becomes over-compressed when the door is closed and exerts too much pressure on the door latch. The proposed design uses a Hall-effect sensor and a permanent magnet in a unipolar, head-on configuration to measure the gap width. Because the relationship between the gap width and sensor output voltage is non-linear, the instrument fits a curve through two calibration data points, and uses this curve to calculate the measured distance from the sensor output voltage. The measurement uncertainty of the instrument was within $\pm 0.5\text{mm}$ over the majority of the desired measurement range, which is within the accuracy range required for this application.

1. Introduction

The door-seal gap width is an important, though often overlooked, specification in the heavy truck industry. The door-seal gap width is the distance between the door opening panel on the truck body and the door itself, in the location where the door-seal will later be installed. This gap has to be adjusted by technicians on the production line to be within specification. If the gap is out of specification, it can cause several issues. A gap that is too large allows water and excessive road noise to enter the truck cabin because the door does not seal properly. A gap that is too small, however, over-compresses the door-seal as the door is closed. This condition requires the operator to apply an excessive amount of force to close the door, which can lead to operator fatigue or discomfort and to excessive wear on other truck components. The over-compressed seal also applies excessive force on the door latching mechanism, which causes the mechanism to wear quickly and possibly fail over time.

No reliable methods currently exist for measuring the door-seal gap. Traditional measuring devices such as calipers and micrometers cannot be used because the gap must be measured while the door is closed. Current methods consist of placing a

piece of clay in the appropriate location on the door opening panel, closing the door on it, opening the door and removing the clay, and then measuring the thickness of the clay. This method is unreliable, however, because the door can over-compress the clay as it closes or, if the clay adheres to the door, can deform the clay as it opens, resulting in an inaccurate measurement. In addition, this measurement is often made before the truck is painted, and the clay can leave residues that adversely affect paint adhesion. This method is also slow, and since it requires the use of clay it is not particularly suitable for a production environment. As a result of these limitations, the door-seal gap width is not currently measured on the production line, and trucks are consequently shipped with doors that are positioned out of specification.

An instrument for measuring the door-seal gap width must satisfy several conditions to be suitable for use on the production line. The instrument must be accurate and reliable. In addition, it must be portable and easy to use so that the measurement can be made as quickly as possible. This paper presents a proof-of-concept design for a proposed instrument that fulfills these requirements. The instrument uses a Hall-effect sensor as

its data acquisition mechanism. A Hall-effect sensor was chosen because it reduces the mechanical complexity of the proposed instrument, is inexpensive, and gives reasonably accurate and repeatable results. The instrument was designed specifically for use on the Freightliner *Cascadia*, which is the current model Class 8 heavy truck manufactured by Freightliner Trucks, a division of Daimler Trucks North America LLC.

2. Theory and Background

In order to take into account all of the necessary considerations in the design of the subject, a basic understanding of the theory behind Hall-effect sensors and their applications is required. This includes an understanding of the basic principle behind the operation of Hall-effect sensors and the effect of magnet orientations on the reading from the sensor.

2.1. Hall-Effect Sensors

A Hall-effect sensor produces an output voltage proportional to the strength of the magnetic field passing through it. These sensors work on the principle of the Hall effect, which acts on a conductor with current flowing through it. When a magnetic field passes through the conductor, it produces a force on the charge carriers (the electrons in a metal or n-type semiconductor) that is perpendicular both to the direction of the magnetic field and to the direction of the current flow. This causes the charge carriers to become concentrated on one side of the conductor, producing an electric potential or voltage. This voltage varies linearly with the magnetic flux density, β , and with the magnitude of the current, I , according to the relationship

$$V_H = \frac{K_H \beta I}{z} \quad (1)$$

where K_H is the Hall constant for the specific conductor and z is the thickness of the conductor. In the case of a Hall-effect sensor, where both K_H and z are fixed, equation (1) can be written as

$$V_H = K \beta I \quad (2)$$

where K is the magnetic sensitivity [1]. The value of K for a specific device is specified by the manufacturer, and is usually given in either volts per gauss or volts per millitesla (mT). From (2), the

strength of the magnetic field can be determined by measuring the Hall voltage V_H .

The sign of the Hall voltage depends on the direction of the magnetic field (*i.e.* if a magnetic field emanating from the north pole of a magnet generates a positive Hall voltage for a specific sensor and configuration, then a magnetic field emanating from the south pole of a magnet will produce a negative Hall voltage for the same sensor and configuration). In addition, because the voltage produced is perpendicular to both the current and the magnetic field, a Hall sensor is sensitive to magnetic fields acting only along one specific axis (in commercially available Hall sensor integrated circuits, this axis is generally perpendicular to the face of the sensor). This axis is referred to as the sensitive axis of the sensor.

2.2. The Effect of Magnet Orientation

Using a Hall-effect sensor to measure displacement poses a special challenge because even though the output voltage of the sensor varies linearly with the magnetic flux density passing through it, this flux density does not vary linearly with the distance from the magnet to the sensor. The displacement of an object is generally measured by placing the sensor in a fixed location, then affixing one or more permanent magnets to the moving object such that the magnets are in close proximity to the sensor.

By varying the combination of the number of permanent magnets and their orientations, the non-linearity of the flux density passing through the sensor with respect to distance can be alleviated to a certain degree. The combinations commonly used in practice generally fall into two sets of categories: head-on vs. slide-by, and unipolar vs. bipolar [1–3]. “Head-on” refers to the condition where the direction of motion of the magnets is parallel to the axis of the magnets’ poles. In this configuration the Hall-effect sensor is placed such that its sensitive axis is coincident with this polar axis. “Slide-by” refers to the condition where the sensor is still placed with its sensitive axis parallel to the axis of the magnets’ poles, but now the direction of motion of the magnets is perpendicular to this axis. In a “unipolar” configuration only one magnet is used, while in a “bipolar” configuration two magnets are used. For the “bipolar head-on” case the sensor is generally placed between the two magnets, and the magnets’ poles are aligned with each other, while in the “bipolar slide-by” case the mag-

nets are placed side-by-side with their poles aligned in opposite directions.

The configuration that tends to yield the most linear relationship between displacement and magnetic flux density passing through the sensor is bipolar slide-by [2]. Due to the geometric constraints for this application, however, it is not feasible to use this configuration. The only feasible configuration for this application is unipolar head-on. In this configuration, the magnetic flux density varies approximately with the inverse square of the distance, d [1]:

$$\beta \propto \frac{1}{d^2} \quad (3)$$

While this relationship is not ideal, a reasonably accurate displacement sensor can still be made using this configuration. McCall and Rohan [4] describe a position transducer that uses this configuration. By using appropriate conditioning circuitry, they were able to obtain a voltage output that was approximately linear with respect to displacement, and that was reasonably accurate at distances of up to 30 to 60mm. A similar approach was taken in the design of the proposed instrument.

2.3. Effect of Magnetic Materials

Ferromagnetic materials such as steel and iron interact with and affect magnetic field lines. One of the ways in which they do this is by redirecting the magnetic field lines. For example, if a ferrous plate is placed between a permanent magnet and a Hall-effect sensor, the magnetic field lines will take the shorter path through the plate and back to the magnetic pole. As a result, the Hall-effect sensor will no longer sense any magnetic field. Another result of this effect is that if a Hall-effect sensor in head-on configuration with a permanent magnet is backed by a piece of ferromagnetic material, the magnetic field that the sensor sees will be intensified [3]. This effect may need to be taken into consideration as many heavy truck bodies are manufactured out of steel.

3. Specifications

The instrument needs to meet several specifications to be suitable for use on the production line. These specifications fit into the categories of geometric requirements, accuracy requirements, human interface requirements, and other miscellaneous specifications. The technical specifications

for the door and requirements for the instrument were obtained in a private communication with a Freightliner engineer [5].

3.1. Geometric Requirements

The instrument must be able to fit entirely within the door-seal gap when the door is closed. Figure 1 shows a CAD model of the door and door opening panel, and Figure 2 shows a typical cross-section of the door, door opening panel, and door-seals. Note that there are two door-seals, and hence two door-seal gaps. The door-seal shown in cyan is the primary door-seal, while the door-seal shown in magenta is the secondary door-seal. Because the door and door opening panels themselves will have been previously checked to verify that they are within specification, it will only be necessary to measure the primary door-seal gap to ensure that both gaps are within specifications.

The instrument would be used by mounting it (using a clip or some other means) on the flat portion of the door opening panel where the primary seal will later be attached (this is the location of the primary seal in Figure 2). The nominal width of the door-seal gap is 15mm, with a tolerance of ± 3 mm. In practice, deviations of up to ± 6 mm may be encountered, which means that the instrument must be able to measure distances ranging from 9 to 21mm. In addition, the height of the instrument, when fully compressed, must be no more than 9mm. The width of the flat portion of the door opening panel on which the instrument will be mounted is approximately 20mm, which defines the maximum allowable width of the instrument. Because the instrument could be placed on relatively straight sections of the door opening, there is no fixed limit on the length of the instrument.

3.2. Accuracy Requirements

Because the tolerance range on the door-seal gap specification is fairly large (± 3 mm), the proposed instrument does not need to be particularly accurate. As long as the absolute error is within approximately ± 0.5 mm, the instrument will be more than accurate enough for the intended application. Because the body of the *Cascadia* is made of aluminum, the effect of ferromagnetic materials such as steel on the accuracy of the instrument does not need to be considered.

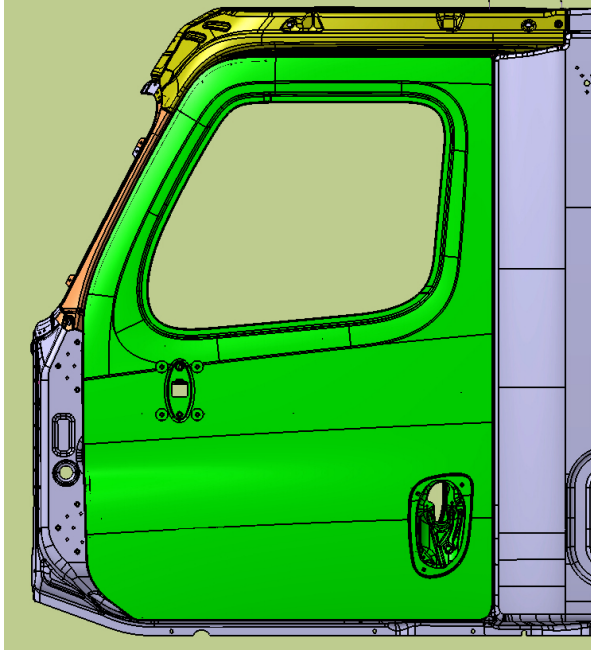


Figure 1: CAD model of the Cascadia's door (green) and door opening panel (gray)

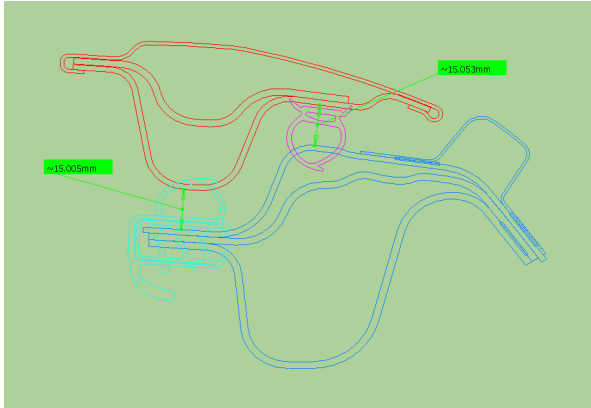


Figure 2: Typical section cut of the door (red), door opening panel (dark blue), primary door-seal (cyan), and secondary door-seal (magenta). The widths of the door-seal gaps are highlighted in green.

3.3. Human Interface Requirements

Technicians would place between 3 and 6 of the proposed instruments at crucial locations around the door opening to acquire the information required to adjust the door properly. The device must therefore be easy to mount on the door opening panel so that technicians can make the measurements quickly. The instrument must also provide some type display that can be read quickly and easily. This would ideally consist of a numerical display that indicates the actual width of the door-seal gap. Because the tolerance range is so large, no more than three significant digits would be necessary on the display. The display should also update in real time.

3.4. Other Requirements

The instrument should be as small and self-contained as possible so that it is easy to use in a production environment. Ideally the instrument would be battery powered, and would either incorporate a display directly onto the instrument or would provide wireless connectivity to eliminate cables. In addition, the instrument should be as inexpensive as possible, which means that it should be easy to manufacture and should use inexpensive components.

4. Methods

There were three main phases to the design of this instrument. The first phase consisted of designing the mechanical and electrical aspects of the instrument and building a physical prototype. The next phase involved designing, implementing, and validating a calibration method. The final phase consisted of collecting data with the device and performing an uncertainty analysis to quantify the accuracy of the instrument.

4.1. Mechanical Design

The final mechanical design of the instrument was chosen for its simplicity. A simple design was chosen to ensure the durability of the instrument and to decrease manufacturing costs. Figure 3 shows a CAD rendering of the proposed design. The instrument consists of a steel arm that is attached at one end to an aluminum base. A plastic or metal clip would be attached to this base so that the instrument can clip onto the door or door opening panel. The Hall-effect sensor is mounted on the

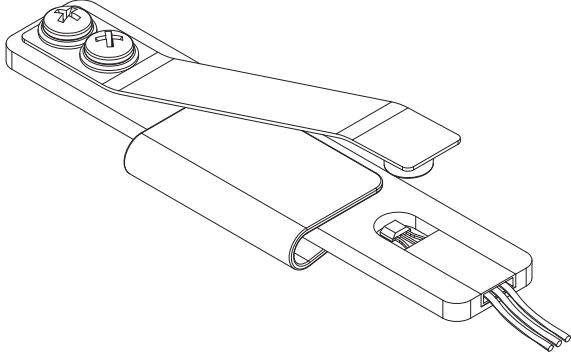


Figure 3: CAD model of the mechanical design of the instrument. The permanent magnet is mounted on the underneath side of the arm such that it is positioned directly above the Hall-effect sensor. Note that the clip can be modified as needed to fit the specific application.

base below the free end of the stainless steel arm, and a permanent magnet is affixed to the free end of the arm. This arm serves as a spring that holds the magnet up away from the sensor. As the instrument is compressed by the door, the arm bends so that the magnet comes into closer proximity to the Hall-effect sensor, and the sensor then produces a corresponding output voltage.

This design does introduce some additional non-linearities into the relationship between the sensor output and the distance being measured. These non-linearities occur because the output voltage of the sensor is sensitive to both translational and angular misalignments of the sensitive axis of the sensor with the polar axis of the magnet. The effect of these irregularities, however, is relatively small and does not significantly affect the accuracy of the instrument. This is demonstrated in Section 5.

4.2. Electrical Design

Because the output voltage of the Hall-effect sensor depends on the magnitude of the power supply voltage, it is essential that the power supply voltage coming into the sensor be consistent. This is accomplished with the filtering circuitry shown in Figure 4. The input voltage to this circuitry would be in the range of 9V, and could come from either a battery or from a wall adapter. The circuitry filters high-frequency noise out of the input, and outputs a constant 5V to the Hall-effect sensor and other electronics. The Hall-Effect sensor chosen for this prototype was the A1302 continuous time, ratiometric, linear Hall effect sensor manufactured by

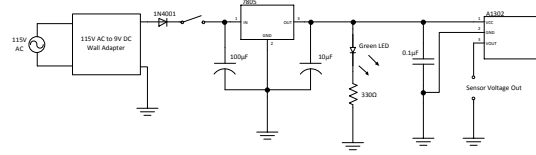


Figure 4: Schematic of the power supply circuitry. An approximately 9V input is connected to the power plug to supply a constant 5V source to the A1302 Hall-effect sensor. The output value is read from pin 3 of the sensor.

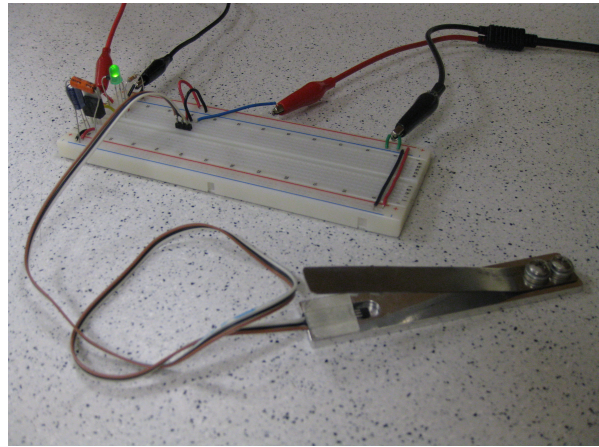


Figure 5: Photograph of the realized hardware implementing the proposed design. The actual measurement device can be seen in the foreground on the right; the power supply circuitry can be seen on the left.

Allegro Microsystems, Inc. (for the full specifications for this sensor, see reference [6]).

Figure 5 shows a photograph of the realized hardware implementing both the proposed mechanical and the proposed electrical design. For the purposes of this proof-of-concept report, all data acquisition and real-time calculations were performed using LabVIEW.

4.3. Calibration

The Hall-effect sensor produces an output voltage that is non-linear with respect to the distance between the sensor and the magnet. A simple curve-fitting method was employed to perform the calibration required to obtain an accurate measurement of the distance from the output voltage from the sensor. This method was chosen because it requires only two data points and so the calibration can be performed very quickly, and because the necessary calculations are relatively simple and so can

be easily implemented on a microprocessor.

From equations (2) and (3), the relationship between the output voltage and the distance being measured is expected to be of the form

$$V = \frac{C}{(d - d_0)^2} + V_Q \quad (4)$$

where C and d_0 are constants to be determined and V_Q is the quiescent output voltage, or the voltage that the Hall-effect sensor outputs when there is no magnetic field present. The value of V_Q is supplied by the manufacturer, and for the A1302 Hall-effect sensor is equal to [6]

$$V_Q = 2.5 \text{ V} \quad (5)$$

Solving equation (4) for d yields

$$d = \frac{C}{\sqrt{V - V_Q}} + d_0 \quad (6)$$

where the arbitrary constant C has been taken outside of the square root. Collecting two data points, (V_1, d_1) and (V_2, d_2) , and substituting them into equation (6) produces the system of equations

$$d_1 = \frac{C}{\sqrt{V_1 - V_Q}} + d_0 \quad (7a)$$

$$d_2 = \frac{C}{\sqrt{V_2 - V_Q}} + d_0 \quad (7b)$$

which needs to be solved for the two unknowns C and d_0 . Subtracting (7b) from (7a) and solving for C gives

$$C = \frac{d_1 - d_2}{\frac{1}{\sqrt{V_1 - V_Q}} - \frac{1}{\sqrt{V_2 - V_Q}}} \quad (8)$$

Solving (7b) for d_0 then yields

$$d_0 = d_2 - \frac{C}{\sqrt{V_2 - V_Q}} \quad (9)$$

where the value of C is obtained from equation (8). For both (8) and (9), the value of V_Q is obtained from (5).

After the calibration is complete, the instrument displays the distance being measured in real time by reading the output voltage from the Hall-effect sensor and plugging it into equation (6) along with the values of C , d_0 , and V_Q . This calibration method was validated by also collecting data points along the entire measuring range of the instrument at intervals of approximately 0.1mm, and then comparing these measured values with the values predicted by the calibration curve fit.

4.4. Effect of Magnetic Materials

In order to gain a basic understanding of how ferromagnetic materials, such as steel and iron, affect the reading of the instrument, a second calibration curve was collected after mounting the instrument on a steel base. This calibration curve was then compared to the original calibration curve. Because the *Cascadia* has an aluminum body, this issue is not particularly relevant and so was not explored in detail. However, this is an issue that should be explored in subsequent design iterations and so it merits at least a mention here.

4.5. Uncertainty Analysis

The sources of error in the proposed measurement system include sensitivity and linearity errors in the Hall-effect sensor, irregularities in the power supply voltage, non-linearities introduced by the mechanical design of the device, errors in data acquisition and digital-to-analog conversion, errors in the calibration equipment, and errors caused by the calibration method itself. A simple uncertainty analysis was performed to quantify the aggregate effect of these sources of error and to provide an estimate of the accuracy of the device.

At 1mm intervals along the entire measurement range of the instrument (9mm to 21mm), sets of 50 data points ($N = 50$) consisting of the measured distances were collected. This was accomplished by repeatedly inserting the device into a fixed gap and recording the measured distance. The mean (\bar{d}) and standard deviation (S_d) of each of these sets was then calculated, and the interval within which—with 95% probability—any single measurement d_i is likely to fall was estimated using the formula

$$d_i = \bar{d} \pm t_{\nu,95} S_d \quad (95\%) \quad (10)$$

where $t_{\nu,95}$ is the Student's-t distribution, and the number of degrees of freedom, ν , is equal to $N - 1$. The term $\pm t_{\nu,95} S_d$ is the uncertainty.

5. Results

There are two main important results obtained from the methods described above: the validation results for the calibration method, and the results from the uncertainty analysis.

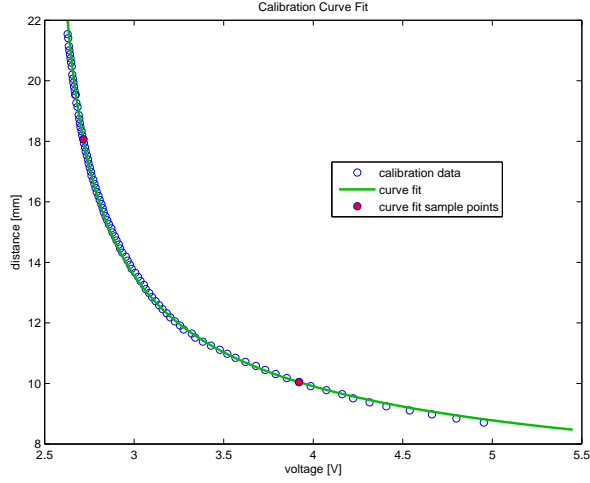


Figure 6: Plot of the recorded calibration data points and the calibration curve fit. The blue points are the individual data points, the green line is the curve fit, and the red points are the data points used for the curve fit. Note that the axes do not start at zero in order to show more detail.

5.1. Calibration

Figure 6 shows the recorded calibration data points along with the curve fit given by equations (6), (8), and (9). Data points were collected at intervals of approximately 0.1mm. The nominal distances of the sample points for equations (8) and (9) were chosen to be 10mm and 18mm. The data points that were actually used are $(V_1, d_1) = (3.9206 \text{ V}, 10.0447 \text{ mm})$ and $(V_2, d_2) = (2.7164 \text{ V}, 18.0647 \text{ mm})$. As can be seen from the figure, equation (6) approximates the actual calibration data very well. There are a few irregularities in the recorded data points compared to the predicted curve; these irregularities are most likely caused by the mechanical design of the instrument as discussed previously.

Figure 7 shows the absolute error between the distance calculated from the output voltage using equation (6) and the distance actually recorded in the calibration points. As is apparent, the error is within the desired $\pm 0.5\text{mm}$ bounds over the entire measurement range, and over the majority of the measurement range the error is within approximately $\pm 0.2\text{mm}$. This result is encouraging, as it suggests that the total final error will likely be within the desired bounds over the majority of the calibration range.

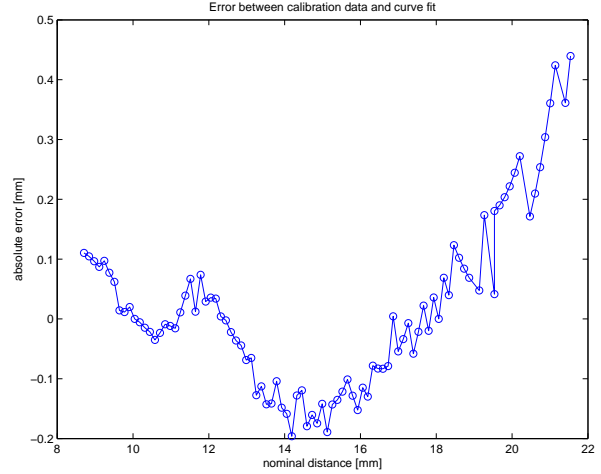


Figure 7: Plot of the absolute error in distance between the calibration data and the estimate given by the curve fit. Note that the axes do not start at zero in order to show more detail.

5.2. Effect of Magnetic Materials

When a steel plate was placed under the base of the instrument, the Hall-effect output voltage changed and the instrument's calibration curve shifted. This new calibration curve is plotted alongside the original calibration curve in Figure 8. As can be seen, there is a significant difference between the two curves. This suggests that at the least the instrument needs to be recalibrated before being used on magnetic materials, or that in future design iterations measures should be taken to eliminate this effect.

5.3. Uncertainty Analysis

Table 1 summarizes the results of the uncertainty analysis calculated from equation (10). These results are also displayed graphically in Figure 9, where the acceptable $\pm 0.5\text{mm}$ error bound is also superimposed. As can be seen, the measured uncertainty is within the $\pm 0.5\text{mm}$ error target over most of the measurement range. The reason for the large uncertainties at 16mm and 17mm is not known, but these results appear to be atypical and non-representative of the accuracy of the instrument in that range. As the nominal distance increases, the uncertainty generally also increases. This is consistent with the calibration curve shown in Figure 6. At small distances, a small change in voltage leads to a very small change in the result of the distance calculation, while at large distances a small change in voltage corresponds to a larger

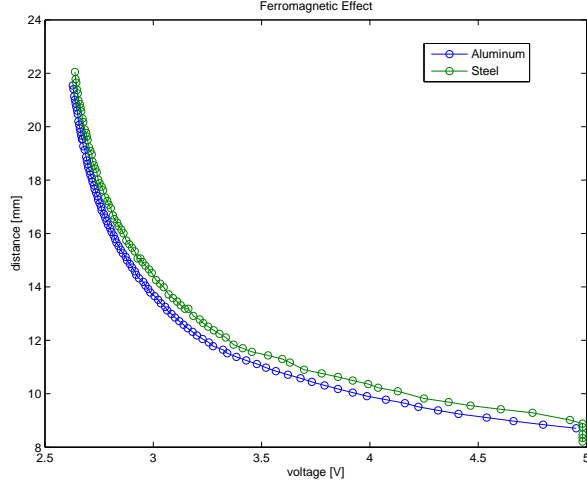


Figure 8: Plot of the calibration curves obtained with an aluminum backing and with a steel backing. Note that the axes do not start at zero in order to show more detail.

nominal distance [mm]	mean [mm]	uncertainty [mm]
9	9.1654	0.039921
10	9.9529	0.056338
11	10.8414	0.059766
12	12.1508	0.015668
13	12.798	0.044167
14	13.6625	0.093894
15	15.0744	0.065627
16	15.533	0.33138
17	16.3714	0.58172
18	18.4192	0.13167
19	18.788	0.4764
20	19.8281	0.72914
21	20.3684	1.2769

Table 1: Mean value and uncertainty range for each of the nominal distances chosen for the uncertainty analysis

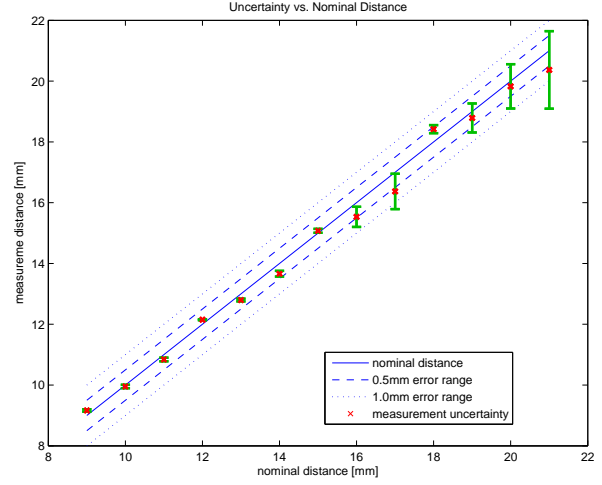


Figure 9: Plot of the results from the uncertainty analysis. The blue lines represent the nominal distance, the $\pm 0.5\text{mm}$ error range, and $\pm 1.0\text{mm}$ error range respectively. The red x's represent the mean values, and the green error bars show the uncertainty.

change in the result. This implies that the accuracy of the instrument is better at smaller distances.

6. Discussion and Conclusions

The proposed design and prototype was successful as a proof-of-concept demonstration for using a Hall-effect sensor based instrument to measure the door-seal gap. The device generally performed well, although there are still a few issues that need to be resolved. In addition, there are still some improvements that should be implemented to make the device ready for commercial use.

The calibration results shown in Figures 6 and 7 demonstrate that the curve-fitting calibration method is reasonably accurate and closely matches the empirical data. In addition, the two-point calibration method can be performed quickly, and is computationally inexpensive and so can easily be implemented using a microprocessor. Furthermore, Figure 9 shows that over the majority of the desired measurement range (9mm to 21mm), the uncertainty associated with the instrument's measurement is within the $\pm 0.5\text{mm}$ error bound target for the device. This level of accuracy obtained with the first prototype suggests that further research and development of this device would be justified.

While the instrument performed well overall, there are still some significant issues that need to be resolved. The first is that at the upper end of

the measurement range (between about 18mm and 21mm), the uncertainty associated with the measurement result increases sharply. Further work needs to be done to resolve this issue. This may include refining the electrical design of the device, or modifying the mechanical design to keep the magnet at a more appropriate distance from the sensor even when large gaps are being measured. Another problem that still needs to be addressed is that the reading from the Hall-effect sensor changes when the instrument is placed on a steel (or any other ferromagnetic) surface. This would obviously be an issue for trucks whose bodies are made of steel. Since the *Cascadia* has an aluminum body, this issue is not immediately relevant. However, it would be worthwhile to conduct further research into solving this issue so that the instrument could be used on truck bodies of any material.

Aside from these major issues, a few minor improvements would still need to be made to transform this prototype design into a commercially viable solution. Certain manufacturing processes could be improved, such as using printed circuit boards and a surface-mount Hall-effect sensor to fix the sensor more securely to the base. In addition, the data processing functionality needs to be implemented on a microprocessor to replace the current LabVIEW implementation. Furthermore, the device should be converted to run on battery power, and could also possibly transmit data using wireless technologies.

While there are still various improvements and refinements to be made, this prototype design functioned extremely well, and serves as a good starting point for developing a commercially viable system for measuring the door-seal gaps on the production line for heavy trucks.

7. Acknowledgments

I would like to thank John Koch for providing technical information and details regarding the requirements for the measurement system. John is a Senior Development Engineer in the Door Systems Integration and Optimization group at Daimler Trucks North America LLC.

References

- [1] D. S. Nyce, *Linear Position Sensors: Theory and Application*. Hoboken, New Jersey: John Wiley & Sons, Inc., 2004.

- [2] D. Ferrazzin, G. Di Domizio, F. Salsedo, C. A. Avizzano, F. Tecchia, and M. Bergamasco, "Hall Effect Sensor-Based Linear Transducer," *Proceedings of the 1999 IEEE International Workshop on Robot and Human Interaction*, vol. 219-224, 1999.
- [3] E. Ramsden, *Hall-Effect Sensors: Theory and Application*, 2nd ed. Amsterdam: Elsevier, 2006.
- [4] W. D. McCall and E. J. Rohan, "A Linear Position Transducer Using a Magnet and Hall Effect Devices," *IEEE Transactions on Instrumentation and Measurement*, vol. 26, no. 2, pp. 133–136, 1977.
- [5] J. G. Koch, Senior Development Engineer, Daimler Trucks North America LLC, Mar. 2012, private communication.
- [6] Allegro MicroSystems, Inc., "A1301 and A1302 Continuous-Time Ratiometric Linear Hall Effect Sensor ICs," datasheet, Worcester, Massachusetts, 2010.